Society of Petroleum Engineers

SPE-213786-MS

Geochemical Impact on Rock Wettability in Injection of High-Concentration Formate Solution for Enhanced Geologic Carbon Storage and Oil Recovery

Oluwafemi Precious Oyenowo, Hao Wang, Ryosuke Okuno, Abouzar Mirzaei-Paiaman, and Kai Sheng, The University of Texas at Austin

Abstract

Aqueous formate (FM) solution has been studied for geologic carbon storage, in which highly concentrated FM solution as carbon-bearing water is injected into the target formation. The literature shows that aqueous FM solution may cause geochemical interactions with carbonate rocks, but no experimental data exist for high-concentration FM solutions. This paper presents a new set of data focused on core-scale wettability alteration of carbonate porous media with varying FM concentration (up to 30 wt%) in NaCl brine. Experimental data from Amott wettability tests and core floods with limestone cores were analyzed to mechanistically understand the wettability alteration observed in the experiments.

Static calcite dissolution tests showed that the degree of calcite dissolution increased with increasing FM concentration in the NaCl brine even with the initially neutral pH. For example, the calcium concentration in the 30-wt% FM case was 15.9 times greater than that in the NaCl brine case with the initial pH of 7.0. Furthermore, reducing the initial solution pH from 7.0 to 6.1 for the 30-wt% FM solution caused the calcium ion concentration to increase by a factor of 3.2. Geochemical modeling indicated that the increased calcite dissolution could be caused by the formation of calcium FM complexes that reduced the activity coefficient of the calcium ion and therefore, drove the calcite dissolution.

The 30-wt% FM solution with the initial pH of 6.1 yielded 4.7 times greater oil recovery than the NaCl brine case in the spontaneous imbibition. The resulting Amott index clearly indicated the wettability alteration to a water-wet state by the FM solution. The 30-wt% FM solution with the initial pH of 7.0 yielded only 30% greater oil recovery than the brine case in the spontaneous imbibition; however, it reached nearly the same amount of total oil recovery (spontaneous and forced) with the 30-wt% FM solution with the initial pH of 6.1. This is likely because the in-situ solution pH could be sufficiently lower than the calcite isoelectric point consistently during the forced imbibition, unlike under the static conditions during the spontaneous imbibition.

Increasing the FM concentration in the injection brine (pH 7.0) delayed the water breakthrough in core floods. Numerical history matching of the core flooding data showed that increasing the FM concentration in the injection brine rendered the initially oil-wet core to a more water-wet state as quantified by Lak and modified Lak wettability indices. Results in this research collectively suggest the importance of in-situ

solution pH in wettability alteration by aqueous FM solution in carbonate media, in order to cause the rock surface to be positively charged in the presence of FM and calcium ions.

Introduction

The world energy outlook (the International Energy Agency, IEA) reported in 2022 that fossil fuels would be a significant part of the energy mix in the coming decades, accounting for over 60% by 2050. Oil and gas represent 75% of the fossil fuel mix (IEA, 2022). In accordance with the Paris Agreement, most countries have set greenhouse gas (GHG) reduction goals of 45% by 2030 and net zero by 2050. CO_2 emissions from burning fossil fuels accounted for about 54% of the global greenhouse gas emissions in 2020 (IEA, 2021). Hence, to meet global GHG emissions targets set by the Paris agreement requires decreasing the carbon intensity of oil and gas production.

Carbonate reservoirs hold approximately 60% of the world's oil reserves (Akbar et al., 2000); hence, it is crucial to reduce the carbon intensity of oil production from these reservoirs. Oil recovery from carbonate reservoirs is affected by the wetting state of the rock among many other factors. Most carbonate reservoirs are mixed/oil-wet because of the adsorption of organic components on the rock surface. Along with fracture networks often present in carbonate reservoirs, this mixed/oil-wet state tends to make the conventional waterflooding without wettability alteration inefficient in improving oil recovery (Anderson, 1986; Harimi et al., 2019; Morrow, 1990).

Different materials have been studied as wettability modifiers in carbonate reservoirs. Wettability modifiers alter the wettability of the carbonate rock through interactions with the rock surface (Standnes and Austad, 2003; Strand et al., 2006; Mahani et al., 2015; Deng et al., 2019; Lara Orozco et al. 2019; Bai et al., 2021; Baghishov et al. 2022). Such wettability modifiers can be categorized largely into surfactants, nanofluids, salts, and alkalis. Ketone solvents as polar solvents (e.g., 3-pentanone) have also been shown to rapidly alter the wettability of carbonate rocks (Wang et al., 2019; Argüelles-Vivas et al., 2020; Wang et al., 2022).

The need to cut back on greenhouse gas emissions resulted in various studies on CO_2-assisted enhanced oil recovery (EOR) techniques, like carbonated-water injection, for wettability alteration (Sohrabi et al., 2011). The carbon storage with these CO_2-assisted EOR techniques has shortcomings associated with CO_2 properties, such as low carbon density at low to moderate pressure, low mass density, low viscosity, low solubility in brine, and corrosivity.

Oyenowo et al. (2023) presented use of an aqueous formate (FM) solution as a carbon carrier for geologic carbon storage. FM ($HCOO^-$) is the simplest carboxylate and the conjugate base of formic acid. FM can be produced via CO_2 electrochemical reduction (CO_2-ECR) (Agarwal et al., 2011; Zhang et al., 2014; Zheng et al., 2017; Philips et al., 2020; Xiang et al., 2020). Most FM salts are highly soluble in water; for example, the solubility of potassium FM at 20°C is 76-wt% (Downs, 1993).

Numerical simulation comparisons between aqueous FM (30-wt% FM) injection and CO_2 injection into an oil reservoir showed that the FM injection resulted in 37% more carbon stored than the CO_2 injection case (Oyenowo et al., 2023). The primary reason for the enhanced carbon storage was the volumetric sweep enhanced by more stable fronts of oil and water displacement by aqueous FM solution than by CO_2. Their cost-revenue analysis showed that CO_2 conversion into FM via ECR for FM injection was economically feasible even at current CO_2-ECR production costs, estimated based on small-scale deployments (Oyenowo et al., 2023).

Recently, the OCEAN (Oxalic acid from CO_2 using Electrochemistry At demonstratioN scale) project demonstrated the viability of the CO_2-ECR technology at an industrial scale, bringing the technology readiness level (TRL) of CO_2-ECR up to 6, and just one level away from field deployment (European Commission CORDIS, 2022). FM is currently produced industrially via the carbonylation of methanol and the hydrolysis of the resulting methyl FM (Hietala et al., 2016), and is readily available at low cost. Decades

of using FM brines in drilling fluid formulations have shown that they have a favorable health, safety, and environmental profile and are compatible with oilfield equipment (Downs, 1993; Howard, 1995).

However, the numerical simulation studies by Oyenowo et al. (2023) did not include geochemical interactions between the solution and the formation. In this research, therefore, we experimentally studied the interactions between FM solutions and carbonates, and the impact of FM injection on the carbonate wettability.

Wang et al. (2023) studied the thermal stability of 20-wt% FM in a brine solution with and without calcite at 85°C. They reported that the FM solution was stable over an aging period of 30 days and the pH of the solutions containing calcite increased due to the calcite dissolution reaction. They visually observed that calcite dissolved more in the FM solution than in brine. Baghishov et al. (2022) studied carboxylate ions, FM, and acetate, as wettability modifiers for carbonate rocks. The FM concentrations in their study were limited to 5-wt% sodium FM (equivalent to 3.3-wt% FM). They found that FM was more effective in altering the wettability of a carbonate core from oil/mixed-wet to water-wet when the solution pH was reduced from about 8.1 to 6.1. Their proposed mechanism of wettability alteration was that pH-induced calcite dissolution released oil from the rock surface, which was followed by adsorption of the FM ion.

Optimizing FM solution injection for carbon storage in carbonates would require injecting high-concentration FM solutions. Increasing the FM concentration is desired for increasing carbon density and also for stabilizing the displacement fronts (oil and formation water) with the increased solution viscosity. However, use of FM concentrations as high as 30-wt% would require a detailed study of the geochemical interactions and the impact on the wettability of carbonate rocks.

Therefore, this research was focused on those geochemical interactions between the FM solution and the carbonate rock and the impact of the FM solution on the wettability. The effect of injecting high concentration FM concentrations (up to 30-wt%) on the carbonate rock was studied using calcite dissolution experiments, contact angle experiments, Amott wettability tests (i.e., spontaneous and forced displacements), and core flooding experiments. Geochemical analysis and numerical history matching of core flooding results were also performed to understand underlying mechanisms involved in the FM injection process.

Materials and methods

This research consists of the experimental and modeling parts. Sections 2.1 – 2.3 explain the materials and methods for the experimental part, and Section 2.4 describes the methods for numerical history matching and geochemical modeling in this research.

Calcite dissolution experiments

The impact of FM concentration in brine on calcite dissolution was investigated using different FM concentrations in NaCl brine: NaCl brine (0-wt% FM) at pH 7.0, 5-wt% FM at pH 7.0, 10-wt% FM at pH 7.0, 20-wt% FM at pH 7.0, 30-wt% FM at pH 7.0, and 30-wt% FM at pH 6.1. The NaCl brine consisted of 5903 ppm Na^+ and 9097 ppm Cl^-. The pHs of the FM solutions were set by adding formic acid. Then, 5 g of synthetic calcite powder was added to glass vials containing 20 ml of these solutions. The mixtures were stirred and put in an oven set at 70°C. The supernatants from these mixtures were collected, and the calcium ion concentrations in the supernatants were measured using inductively coupled plasma mass spectrometry (ICP-MS).

Amott wettability tests

Amott wettability tests, consisting of spontaneous and forced displacements, were performed using Texas Cream limestone cores. Four aqueous solutions were selected out of the six solutions mentioned in Section 2.1. Table 1 lists the mass densities for the four solutions: NaCl brine, 5-wt% FM solution at pH 7.0, 30-wt% FM solution at pH 7.0, and 30-wt% FM solution at pH 6.1. The pH values refer to the initial solution

pH, which varied during the experiments. Table 1 also gives the interfacial tension (IFT) values measured for the aqueous solutions with the oil used for the experiment (Table 2), and the core properties measured in this research.

Table 1—Mass densities and IFTs with the Texas crude (Table 2) for the aqueous solutions, and properties of the Texas Cream Limestone cores used in the Amott wettability tests (Section 2.2).

	Brine case	5-wt% FM case (pH 7.0)	30-wt% FM case (pH 7.0)	30-wt% FM case (pH 6.1)
Solution density, kg/m^3	980	1030	1296	1296
Oleic/Aqueous phase IFT, mN/m	7.37 ± 0.08	6.01 ± 0.07	2.76 ± 0.04	3.07 ± 0.08
Inverse Bond number	67.1	33.3	7.5	10.1
Core height, cm	11.8	12.1	12.3	12.1
Core diameter, cm	3.7	3.7	3.7	3.8
Porosity, %	32.1	32.7	31.0	30.5
Permeability, md	10.2	17.6	16.1	11.2
Initial oil saturation, %	55.4	57.7	56.1	61.2
Pore volume, ml	40.7	42.4	41.0	41.9
OOIP, ml	22.57	24.45	23.00	25.64

Table 2—Oil composition and properties.

Components	Mass percent
C_3	0.1%
C_4	0.4%
C_5	1.5%
C_6	3.0%
C_7	4.8%
C_8	6.5%
C_9	5.6%
C_{10}	5.2%
C_{11}	4.1%
C_{12}	4.0%
C_{13}	4.1%
C_{14}	3.7%
C_{15+}	57.0%
Relative molecular weight, g/mol	183
Density, kg/m^3	795 (at 22°C)
	770 (at 70°C)
Viscosity, cp	2.7 (at 22°C)

The cores were initially saturated with brine, and then with oil at room temperature. Afterwards, the cores were aged in oil for 12 weeks (6 weeks at 70°C followed by 6 weeks at room temperature). Subsequently, the oil was injected again into the cores to have a more uniform fluid distribution and make sure that the cores were at their residual water saturation.

Spontaneous imbibition. The solutions to be tested were prepared and placed in an oven, set at 70°C (the experiment temperature), for 24 hours. Amott cells were cleaned and calibrated to make sure the graduations on the cells were consistent with the labels. The oil saturated cores were placed in the Amott cells, which contained the respective solutions. To minimize the effect of fluid expansion, both the cells and the solutions were set up at 70°C (see Figure 1 for a picture of the spontaneous imbibition setup). Amott cells were placed in the oven at 70°C for the duration of the experiment. The oil recovery was recorded periodically by measuring the amount of the oil collected at the top of Amott cell as shown in Figure 1. The calcium ion concentrations in the solutions after spontaneous imbibition were measured using ICP-MS.

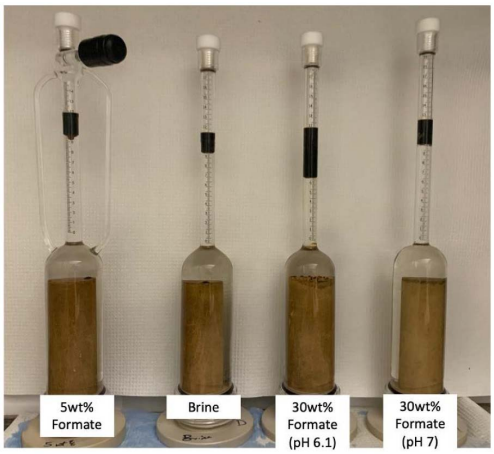

Figure 1—Amott cells for the four cases of spontaneous imbibition (Section 2.2.1).

Forced imbibition. After the spontaneous imbibition, the cores underwent forced oil displacement by the respective aqueous solution. Figure 2 shows a schematic of the experimental setup used. The setup consisted of a pressurization pump (Teledyne ISCO 100 DX), a hydraulic pressure pump (ENERPAC P-391) to provide overburden pressure, an accumulator for the injection solution, a Hassler-type core holder, 2 way-valves, and an oven for maintaining the system temperature at 70°C.

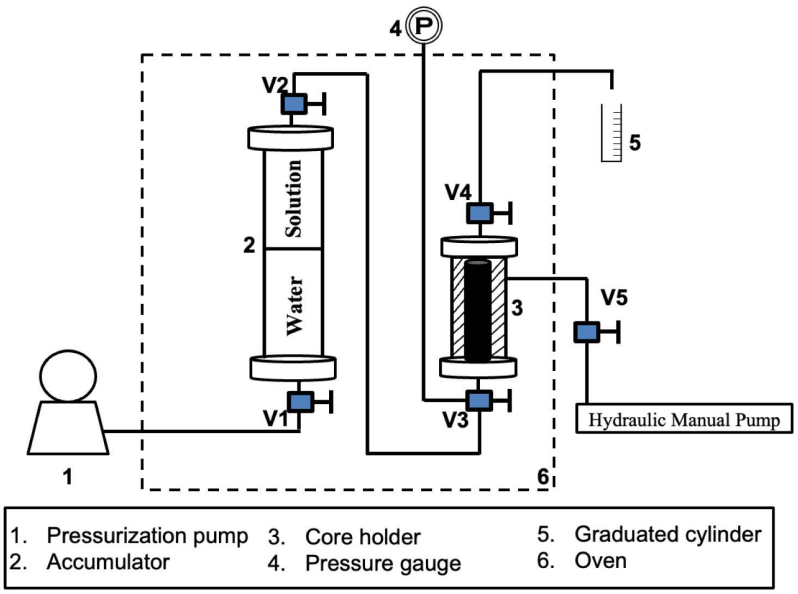

Figure 2—Schematic for the experimental set up for the forced imbibition (Section 2.2.2)

Core flooding was started by injection of the respective solution at a constant rate of 40 ml/hr. The injection rate was set such that the critical capillary number of 2×10^{-5} was not exceeded as explained in the next section. The capillary number, N_{vc}, is a dimensionless ratio of viscous to capillary forces. The most fundamental form of capillary number is

$$N_{vc} = \frac{K \Delta P}{\sigma L} \quad (1)$$

where K is permeability, ΔP is differential pressure across the flow distance (L), and σ is the oil/water interfacial tension (Lake et al., 2014).

After water cut reached 100%, the injection flow rate was increased from 40 to 200 ml/hr to minimize the capillary end effect on the final fluid saturations. The injection rate was increased so that the Rapoport and Leas number N_{RL} of 3 cp-cm^2/min was exceeded (Lake et al., 2014; Rapoport and Leas, 1953):

$$N_{RL} = Lu\mu \quad (2)$$

where L is the length of the core in centimeters, u is the superficial velocity in cm/min, and μ is the injected fluid viscosity in cp. The produced fluids were collected in graduated vials to calculate oil recovery.

Core flooding

Indiana limestone cores were used for the core-flood experiments. The cores were 2.54 cm in diameter and 22.86 cm in length. The porosities and permeabilities of the cores were measured with brine in the core-flood system. Then, oil was injected into the core to establish the initial oil saturation, which was calculated by the volume of produced brine. During the oil injection process, the pressure drop was measured by a pressure transducer to estimate the end-point relative permeability of oil.

Core floods were carried out with the brine, 20-wt% FM, and 30-wt% FM solutions at room temperature with all initial pH values of 7.0. Table 3 summarizes the experimental conditions. The viscosity ratio shown in Table 3 is the ratio of the viscosity of oil to that of the injection fluid. The injection rate was designed based on the capillary number (N_{vc}). According to Lake et al. (2014), the residual oil saturation is independent of capillary number at low capillary number; however, the residual oil saturation begins to decrease when capillary number becomes greater than critical capillary number $(N_{vc})_c$. In this experiment, therefore, a low capillary number was designed for all three core floods. Injection rates for FM cases were smaller than brine case because of higher viscosity of FM solution than brine. Injection fluids were injected for about 1.5 pore volumes. The effluent samples were collected in plastic graduated vials. The volumes of oil and water phases were measured to calculate oil recovery.

Table 3—Experimental conditions for core flooding tests with Indiana limestone cores

Experiment	Brine Case (pH 7)	20-wt% FM Case (pH 7)	30-wt% FM Case (pH 7)
Porosity, %	22.07	22.36	21.58
Permeability, mD	44.66	53.24	45.57
Pore volume, ml	25.56	25.90	25.00
Initial oil saturation, %	50.86	52.42	52.05
Viscosity of injected fluid, cp	1.0	3.3	8.3
Viscosity ratio	2.70	0.82	0.33
Injection rate, ml/hour	12.00	3.64	1.45
Capillary number	6.47×10^{-7}	3.02×10^{-6}	2.04×10^{-6}

Results of core flooding tests were history-matched by numerical simulation to quantify the wettability alteration by using the calibrated relative permeabilities as will be explained in Section 2.4.2. Note that the

FM solutions were more viscous than the brine as shown in Table 3, leading to an increased displacement efficiency according to the Buckley-Leverett theory (Oyenowo et al. 2023).

Simulation and modeling

Geochemistry modelling using PHREEQC. Geochemical reaction models in the PHREEQC software (Parkhurst and Appelo, 2013) were used to mechanistically understand the interactions between the FM solution and calcite. PHREEQC can simulate dissolution reactions of minerals in aqueous solutions by employing principles of equilibrium chemistry between aqueous solutions and minerals.

The solubility of a mineral in a solution is expressed as a mass-action equation with a temperature-dependent equilibrium constant. For example, the dissolution of calcite is written as $CaCO_{3\,(s)} \rightarrow Ca^{2+}_{(aq)} + CO^{2-}_{3\,(aq)}$ with the equilibrium constant $\log_{10}K_{25°C} = -8.48$. The resulting mass-action expression is

$$K_{25°C} = 10^{-8.48} = \frac{a_{Ca2+}\, a_{CO_3^{2-}}}{a_{CaCo_3}} \tag{3}$$

where a_x is the activity of component x in solution. The activity, a_x, is defined as a product of the molar concentration of component x and the activity coefficient of component x, in solution. The activity of a pure solid is 1.0 by convention.

PHREEQC uses the mass-action equation for solubility to model the ionic concentrations based on the activity coefficient of the ions and the properties of the solution. In this research, the compositions of the aqueous solution were defined and used as input in the equilibrium models. Then, PHREEQC estimated the activity coefficient of each ion in solution.

The activities of ions in solution depend on long-range electrostatic forces and short-range interionic forces within the solution. Ions in solution form complexes with each other, which affect the activity of ions (Clegg, 2018). Accurate estimation of the activity coefficient by PHREEQC requires defining the ion complexation reactions and choosing the appropriate activity coefficient model.

PHREEQC has two models that account for short-range and non-electrostatic interactions, which are important in highly concentrated solutions. They are the Pitzer model contained in the pitzer.dat database, and the specific ion interaction theory (SIT) model contained in the sit.dat database. The Pitzer equation is a rigorous model that describes the ion-interactions in solutions; however, several ion-specific parameters are not currently available for FM ions (Pitzer, 1991). For this research, therefore, the simpler SIT activity coefficient model was implemented by using the sit.dat database in PHREEQC.

Thermodynamic data on FM were obtained from PHREEQC minteq.v4 database (Allison et al., 1990; U.S. Environmental Protection Agency, 1998). Calcium can form both unidentate and bidentate complexes with FM, yielding the positively charged calcium monoformate ($CaHCOO^{+}_{(aq)}$) and the neutral charged calcium biformate ($Ca(HCOO)^{0}_{2\,(aq)}$), respectively (Carrell et al., 1988; Deerfield et al., 1989).

The chemical equations for the formation of the calcium-FM complexes were added to the model, for a better description of the aqueous system.

$$Ca^{2+} + HCOO^{-} \rightarrow CaHCOO^{+}_{(aq)} \log_{10}K = -1.43 \tag{4}$$

$$Ca^{2+} + 2HCOO^{-} \rightarrow Ca(HCOO)^{0}_{2\,(aq)} \log_{10}K = -2.24 \tag{5}$$

The stability constant for the calcium monoformate ion complex was used from the MINTEQ database while the stability constant for the calcium biformate ion complex was read from Giebson et al. (2010). After defining the complexation reaction, the solubility product of the calcium FM salt was estimated by matching the solubility data provided in the IUPAC-NIST solubility database using PHREEQC.

The dissolution of calcite leads to the formation of CO_2. Because the vials used in the calcite dissolution experiment were closed, the CO_2 pressure in the vials should not be the partial pressure in air at atmospheric pressure. Since the activity-coefficient model is accurate at low concentrations, we estimated the CO_2 partial pressure by matching the measured calcium ion concentration in brine and assumed that the CO_2 partial pressure was the same for all other solutions.

The enthalpy of formation for the calcium biformate complex was estimated by matching the measured calcium concentration in the 5-wt% FM solution. After the calibration was done, the model was then used to estimate the calcium ion concentrations in the different solutions and compared with the measured concentrations from the calcium dissolution experiment (see Appendix A for PHREEQC input script).

History matching of core flooding tests. Core flooding results were numerically history-matched using CMG IMEX (Computer Modelling Group, 2020). Mercury injection capillary pressure (MICP) data showed that Indiana limestone cores present a bimodal pore-size distribution (Alarji et al., 2022). As shown in Figure 3, therefore, the numerical simulation model consisted of two layers with different permeabilities and cross-sectional areas, which yielded additional flexibility in history matching.

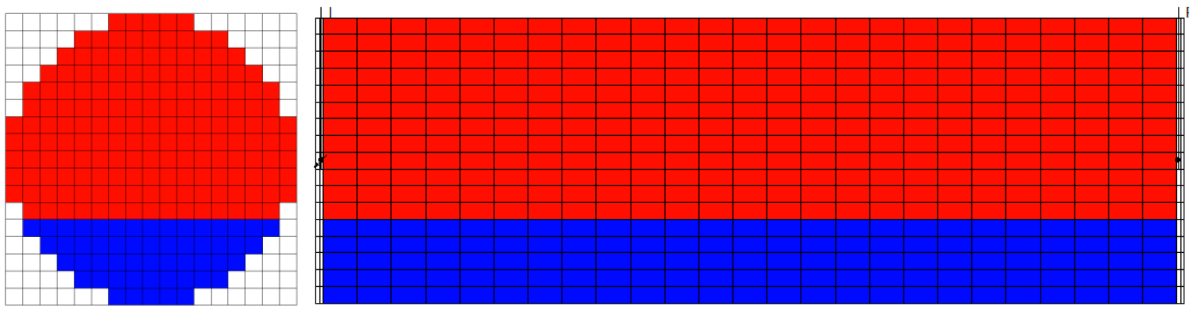

Figure 3—Numerical simulation model for history matching of core flooding results (Section 2.4.2): (a) I-K cross-section, (b) J-K cross-section. The high permeability layer is in red and the low permeability layer is in blue. There are 17 gridblocks in the I direction, 101 gridblocks in the J direction, and 17 gridblocks in the K direction. The gridblocks have the dimension of 0.15 cm × 0.24 cm × 0.15 cm (I × J × K).

Table 4 shows the simulation settings and parameters for each solution injection model after history matching. The history matching consisted of two steps. The first step was to adjust the permeability and area for each layer to match the oil recovery. The flow capacity (product of permeability and area) ratio for each model was fixed at 17 to ensure the same level of tendency for channeling flow at the core scale. The average permeability for each core was the same as absolute permeability measured by brine before the core-flood experiments.

Table 4—Parameters for two layers in the history matching of core flooding results (section 2.4.2). The three solutions had the initial pH of 7.0.

	K_1A_1 / K_2A_2	K_1, mD	A_1 area %	K_2, mD	Average K, mD
Brine	17	55	76.0	11	45
20-wt% FM	17	57	88.7	26	53
30-wt % FM	17	46	97.3	39	46

The second step was to adjust relative permeability curves to match the water breakthrough and oil production. Then, the wettability alteration by FM was quantified by Lak wettability index and modified Lak wettability index. Lak wettability index is defined as (Mirzaei-Paiaman, 2021):

$$I_L = \frac{A\left(0.3 - k_{rw,Sor}\right)}{0.3} + \frac{B\left(0.5 - k_{rw,Sor}\right)}{0.5} + \frac{CS - RCS}{1 - S_{or} - S_{wc}} \quad (6)$$

where I_L is Lak wettability index, which ranges from –1.0 to 1.0, $k_{rw,Sor}$ is the water relative permeability at residual oil saturation, CS is the intersection saturation point of oil and water relative permeability curves, and RCS is the reference crossover saturation defined as

$$RCS = 0.5 + \frac{S_{wc} - S_{or}}{2} \quad (7)$$

S_{or} and S_{wc} are the residual oil saturation and irreducible water saturation, respectively; A and B are two coefficients defined as

A=0.5 and B=0.0, if $k_{rw,Sor}<0.3$

A=0.0 and B=0.0, if $0.3 \leq k_{rw,Sor} \leq 0.5$

A=0.0 and B=0.5, if $k_{rw,Sor}>0.5$

We note that to use Lak wettability index, relative permeability is defined as effective permeability divided by oil permeability at initial water saturation.

Modified Lak wettability index is defined as (Mirzaei-Paiaman et al., 2022)

$$I_{ML} = \frac{A_o - A_w}{A_o + A_w} \quad (8)$$

where $I_{ML}$is modified Lak wettability index; A_o and A_w are the areas below the oil and water relative permeability curves, respectively.

Results and Discussion

This section presents results from the experiments described in the previous section. A mechanistic analysis is given to the wettability alteration observed in the core-scale experiments, such as Amott wettability tests and core flooding.

Calcite dissolution measurements and geochemical simulation

Figure 4 shows the calcite level in the tested solutions after 24 hours. The brine used in preparing the FM solution did not contain any calcium ions; hence, any calcium ion in the solution was from dissolved calcite. Figure 5 shows the calcium ion concentrations measured from these solutions. The marginal variations in this figure mean that the calcite dissolution occurred rapidly, mostly within a day, in the solutions. Figure 6 compares the calcium ion concentrations for the tested solutions. Increasing the FM concentration increased the amount of calcite dissolved in the solution, even at the initial pH of 7.0 as seen for the brine and FM solutions (5-wt% – 30-wt%). For example, the calcium concentration in 30-wt% FM was 15.9 times greater than that in the brine with the initial pH of 7.0. Also, comparison between the two 30-wt% FM solutions indicates that reducing the initial solution pH from 7.0 to 6.1 caused the calcium ion concentration to increase by a factor of 3.2.

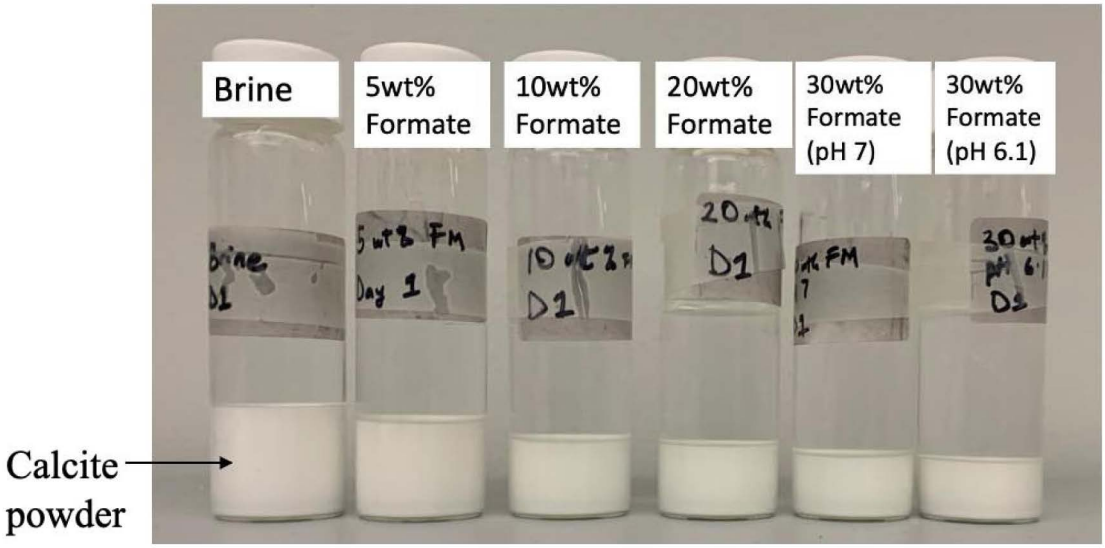

Figure 4—Snapshot of the calcite dissolution experiment in different aqueous solutions after 24 hours.

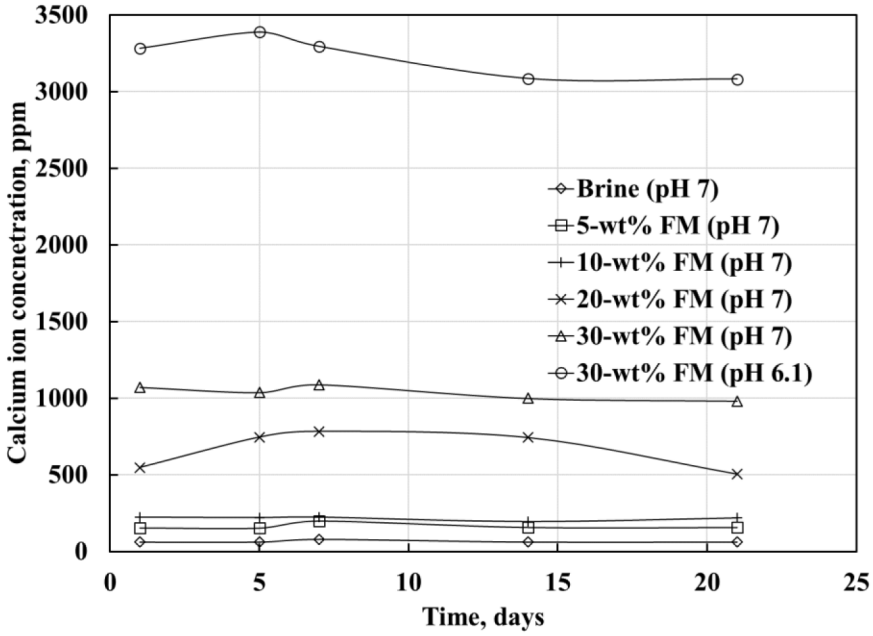

Figure 5—Calcium ion concentrations measured for different aqueous solutions after aging with calcite (Section 3.1).

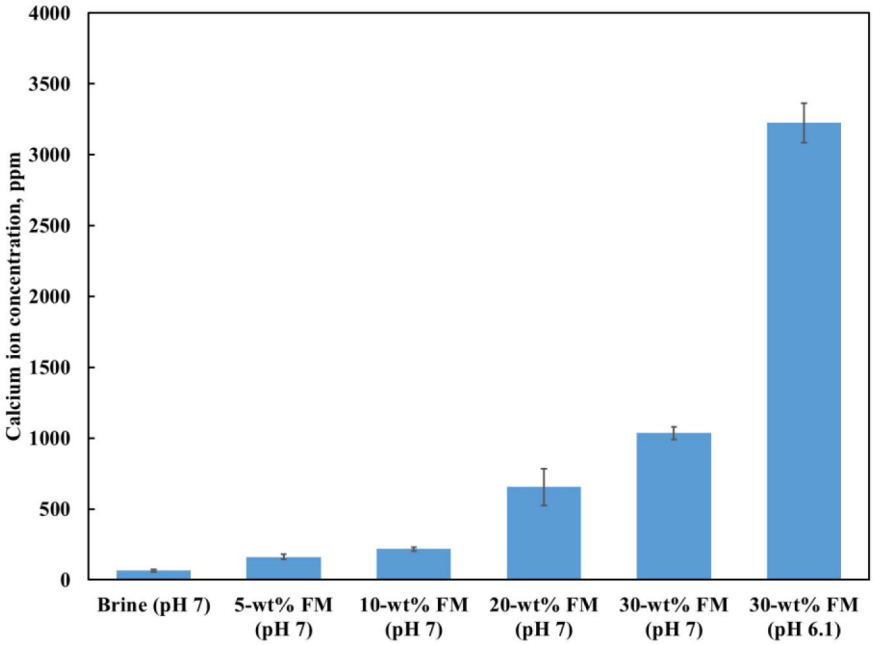

Figure 6—Average calcium ion concentration in each solution after calcite dissolution experiment (Section 3.1).

Figure 7 compares the calcium ion concentration measured from the calcite dissolution experiment and from the PHREEQC geochemical model. The model was in good agreement with the experimental data except for the 30-wt% FM at the initial pH of 6.1. The substantial deviation observed for this solution likely came from the elevated level of calcite dissolution and complexity in the associated reactions.

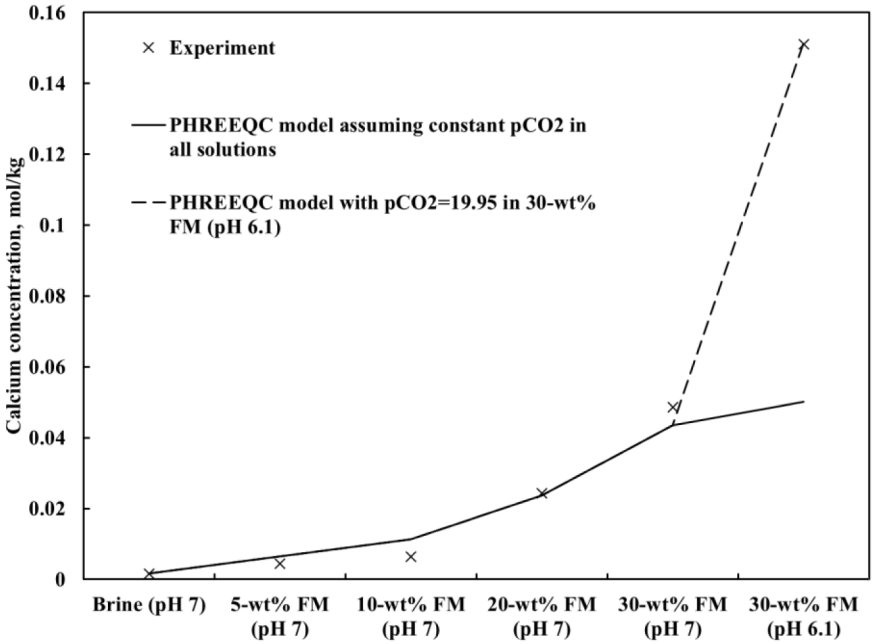

Figure 7—Calcium ion concentrations from PHREEQC and from direct measurements using ICP-MS (Section 3.1).

An initial attempt to investigate into the deviation for the 30-wt% FM solution (pH 6.1) was to back calculate the CO_2 partial pressure that matches the calcium concentration data. Because the systems were closed, it is conceivable that the CO_2 partial pressure increased with an increased amount of dissolved calcite. However, to match the calcite concentration in the 30-wt% FM (pH 6.1) required the CO_2 partial pressure

for the 30-wt% FM solution (pH 6.1) to increase to 20 atm, which is unrealistically large. Therefore, the CO_2 partial pressure alone does not explain the deviation observed for this solution in Figure 7.

Another potential reason for the inaccurate result for the 30-wt% FM solution (pH 6.1) in Figure 7 is that the activity coefficient model could not describe the effect of hydrogen ion activity on ionic interactions in the solution, leading to inaccurate estimations of the aqueous species activity coefficients. A more detailed description of the FM solution and the ionic interactions is necessary for accurate descriptions of highly concentrated FM solutions. The development of such models, though beyond the scope of this study, will be important for modeling of aqueous FM solutions at high concentrations.

The aqueous speciation in PHREEQC showed that calcium in the solution existed predominantly (approximately 90%) as $CaHCOO^{+}_{(aq)}$ and $Ca(HCOO)_{2\,(aq)}$ complexes. These calcium and FM complexes reduce the activity coefficient of the calcium ion, and therefore, increase the molar concentration of dissolved calcite. Therefore, increasing the FM concentration in the solution tends to increase the formation of calcium-FM complexes, which consequently increases the amount of calcite dissolved. Then, the next sections will address a question as to how the elevated level of calcite dissolution affected the static and dynamic core-scale experiments, Amott tests and core flooding, in this research.

Amott test

Figure 8 shows the oil recoveries from the spontaneous imbibition experiments. The data were scaled using the Leverett radius, $\sqrt{k/\phi}$, to account for differences in the pore structure among the different cores used (Mason and Morrow, 2013; Mirzaei-Paiaman and Masihi, 2013; Mirzaei-Paiaman et al., 2017). The 30-wt % FM solution with the initial pH of 6.1 yielded the highest oil recovery, 23% pore volume (PV), which was much greater than the other solutions tested. The oil recoveries from the other three solutions were 5.3%, 6.1%, and 6.8% PV for the brine, 5-wt% FM, and 30-wt% FM (pH 7.0) solutions, respectively.

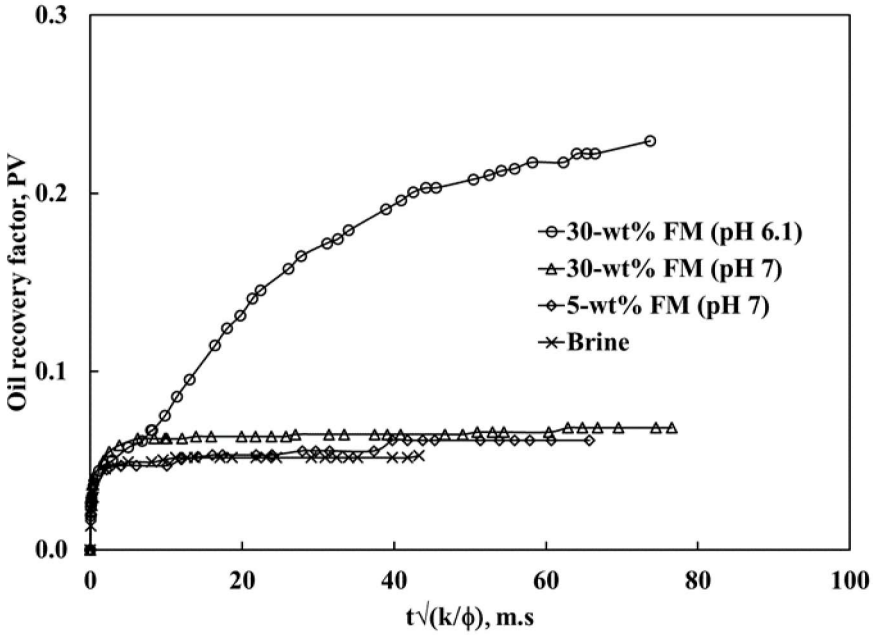

Figure 8—Oil recoveries from spontaneous imbibition experiments in terms of pore volume (PV). The 30-wt% FM solution with the initial solution pH of 6.1 gave a marked different oil recovery curve from the other three cases. Results are explained in Section 3.2.

Capillary and gravity forces are important for oil recovery during the spontaneous oil displacement by water (Gupta and Mohanty, 2010; Meng et al., 2016; Mirzaei-Paiaman, 2015; Rostami Ravari et al., 2011). The relative contribution of these two forces is described by the inverse Bond number, N_B^{-1}.

$$N_B^{-1} = C\frac{\sigma\sqrt{\phi/k}}{\Delta\rho g H} \tag{9}$$

where C is 0.4 for the capillary tube model, σ is the oleic/aqueous phase interfacial tension in N/m, φ is porosity, k is permeability in m^2, $\Delta\rho$ is the density difference between the aqueous and oleic phases in kg/m^3, g is acceleration due to gravity in m/s^2, and H is the height of the core in m. Capillary dominant flow is when $N_B^{-1} > 5$ (Schechter et al., 1994). N_B^{-1} ranged from 7.5 to 67.1 in our displacements (Table 1), indicating capillary dominant flow as is often the case with core-scale experiments.

To interpret the spontaneous imbibition results, we note that the cores had similar initial water saturations (ranging from 39 to 45%), porosities, and permeabilities. Table 1 shows the oleic/aqueous phase IFT for the solutions. The result shows that increasing the FM concentration caused a slight reduction in IFT. The 30-wt % FM solutions at different initial pH values, 6.1 and 7.0, had similar IFT values, but resulted in markedly different oil recoveries (Figure 8). Therefore, the slight IFT reduction with the 30-wt% FM solution (pH 6.1) should not have had a significant contribution to the observed oil recovery.

The calcite dissolution experiment (section 3.1) showed that increasing FM concentration enhanced the level of calcite dissolution, which by itself could be responsible for wettability alteration in carbonates (Hiorth et al., 2010). Figure 9 shows the oil recovery after the spontaneous imbibition process and the respective calcium ion concentration in the solution. As expected, the calcium ion concentration increased with increasing FM concentration, because of more dissolution of calcite. However, the oil recovery was quite incentive to the level of calcite dissolution for the three FM concentrations at the initial solution pH of 7.0. The 30-wt% FM solution at the initial solution pH of 6.1 yielded a much greater level of calcite dissolution and oil recovery via spontaneous imbibition.

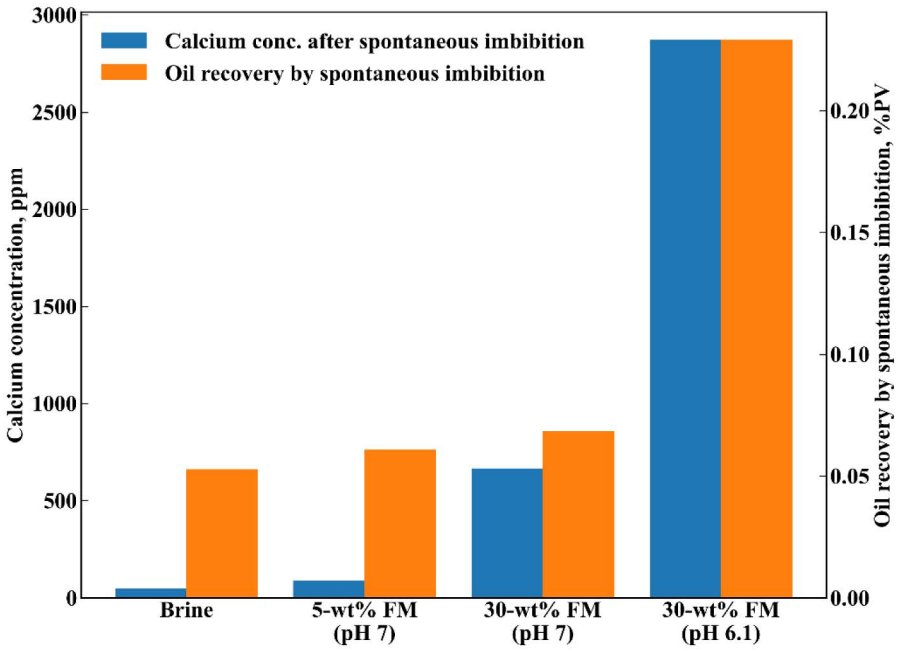

Figure 9—Oil recoveries by spontaneous imbibition and calcium ion concentrations in the solutions after spontaneous imbibition (Section 3.2). The 30-wt% FM solution with the initial solution pH of 6.1 gave a much greater level of calcite dissolution and oil recovery.

Previous studies showed that the solution pH and the concentration of potential determining ions (PDI) affected the charge of the carbonate surface (Somasundaran and Agar, 1967; Al Mahrouqi et al., 2017; Zeng et al., 2020). Ca^{2+}, Mg^{2+}, CO_3^{2-}, and SO_4^{2-} are recognized as PDI in the carbonate system (Somasundaran and Agar, 1967; Strand et al., 2006; Zhang and Austad, 2006). The brine used for Amott test was NaCl

brine, but NaCl does not dictate the surface potential in carbonates (Pierre et al., 1990; Strand et al., 2006). Therefore, the only PDI present in the solution, Ca^{2+} and CO_3^{2-}, were generated by the calcite dissolution in this research.

The speciation of CO_3^{2-} ions depends on the solution pH. High solution pH values above 8 favor the speciation of carbonate ions (CO_3^{2-}), while the lower pH values favor bicarbonate and carbonic acid speciation. In solutions with pH < 8, an abundance of calcium ions over carbonate ions in solution tends to cause the surface to be positively charged. The isoelectric point of calcite, at which the calcite surface has a net neutral charge, was experimentally determined to be 8.2 in pH by Somasundaran and Agar (1967).

Table 5 shows the pH values and calcium ion concentrations of the solutions after the spontaneous imbibition experiments. The pHs of the brine, 5-wt% FM, and 30-wt% FM solutions with the initial pH of 7.0 increased to approximately 8.5 through the spontaneous imbibition experiment. For the 30-wt% FM solution with the initial pH of 6.1, however, it only increased to 6.55. That is, the solution pH was much lower than the isoelectric point of calcite throughout the experiment for the 30-wt% FM (pH 6.1). The low pH and the calcium ion concentrations from the dissolved calcite likely kept the calcite surface positively charged. Therefore, we hypothesize that the high oil recovery by the 30-wt% FM solution with the initial pH of 6.1 came mainly from the wettability alteration caused synergistically through calcite dissolution, the solution pH sufficiently lower than the isoelectric point of calcite, and subsequent geochemical interactions.

Table 5—pH and calcium ion concentration in solution after spontaneous imbibition (Section 3.2).

Solution	pH of solution after spontaneous imbibition	Calcium ion concentration, ppm
Brine (initial pH 7.0)	8.54	47.8
5-wt% FM (initial pH 7.0)	8.71	88.6
30-wt% FM (initial pH 7.0)	8.38	667.2
30-wt% FM (initial pH 6.1)	6.55	2872.2

Figure 10 shows the total oil recoveries in the Amott wettability experiments (both spontaneous and forced displacements). The oil recoveries at "0 PVI" in this figure are those from the spontaneous imbibition. For all the solutions, the oil recovery leveled off after 5 pore-volumes injected (PVI). The total oil recoveries by the brine, 5-wt% FM, 30-wt% FM (the initial pH 7.0), and 30-wt% FM (the initial pH 6.1) were 0.41, 0.42, 0.56, and 0.58 PV, respectively.

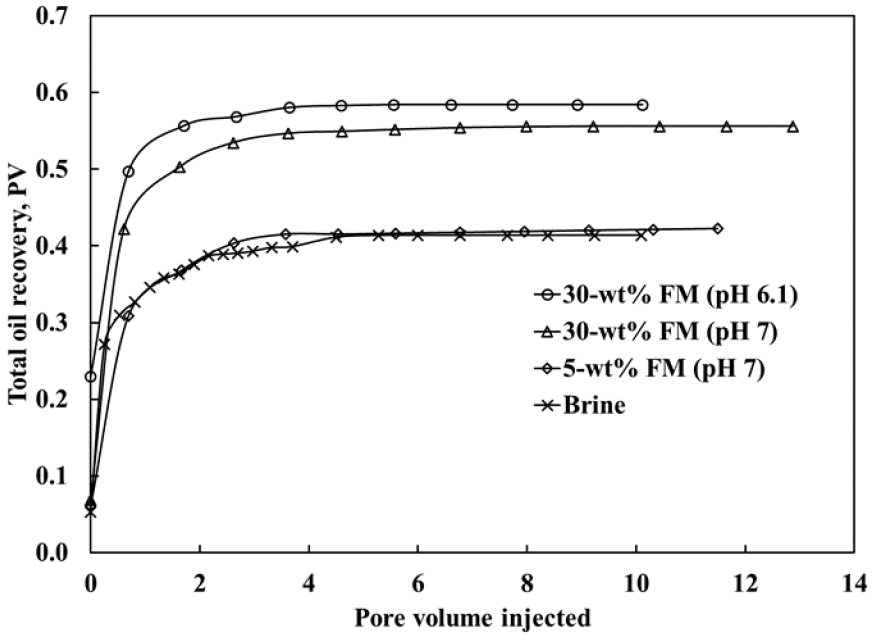

Figure 10—Total cumulative oil recoveries from the Amott wettability experiments (both spontaneous and forced displacements) as explained in Section 3.2. The "0 PVI" intercept on the vertical axis corresponds to the oil recovery from the spontaneous imbibition experiment.

Table 6 shows that the 30-wt% FM solution with the initial pH of 7.0 recovered 22.78 ml of oil, and that with the initial pH of 6.1 recovered 24.45 ml in total. They were approximately 90% of their initial amounts of oil in the core. However, Table 6 indicates that they likely had different mechanisms of oil recovery because the Amott index for the 30-wt% FM solution (pH 6.1) was nearly three times greater than those for the other solutions. The results clearly show that the 30-wt% FM solution (pH 6.1) caused a change in the core wettability, but the 30-wt% FM solution with pH 7.0 did not. This observation highlights the importance of the solution pH in the wettability alteration by aqueous FM solution. This is consistent with Baghishov et al. (2022), in which the 5-wt% FM solution with the initial pH of 6.1 resulted in wettability alteration of calcite-rich shale, but the straight brine without FM with the same initial pH did not.

Table 6—Amott indices to water for all solutions tested (Section 3.2). The 30-wt% FM solution with the initial pH of 6.1 resulted in a much greater Amott index than the other solutions tested.

Case	Oil recovery from spontaneous imbibition, ml	Oil recovery from forced imbibition, ml	Amott index to water
Brine (initial pH 7.0)	2.15	14.70	0.1276
5-wt% FM (initial pH 7.0)	2.60	15.31	0.1452
30-wt% FM (initial pH 7.0)	2.80	19.98	0.1229
30-wt% FM (initial pH 6.1)	9.60	14.85	0.3926

As shown in Figure 6, the 30-wt% FM solution with the initial pH of 7.0 dissolved 15.9 times more calcite than the brine in the static calcite dissolution experiments (section 3.1). It is possible that the total oil recovery by the 30-wt% FM (pH 7.0) was impacted by changes in pore structure caused by calcite dissolution. Also, the pH change and the associated reactions during the experiment could have contributed to the observed oil recovery. Although calcite dissolution must have occurred during the forced displacement, the pH should not have become as high as those recorded in the spontaneous imbibition experiments because an equilibrium state was not possible under the dynamic conditions. Hence, the 30-

wt% FM solution with the initial pH of 7.0 may have had similar mechanisms in effect to the other 30-wt % FM solution with the initial pH of 6.1.

This implies the potential shortcoming of Amott wettability test, where the spontaneous and forced displacement may have different solution pH values relative to the calcite isoelectric point. In particular, Amott wettability index can substantially underestimate the 30-wt% FM solution with the initial pH of 7.0 as a wettability alteration agent for EOR since its oil recovery from carbonate cores is sensitive to the in-situ solution pH with respect to the calcite isoelectric point. Therefore, the next section presents the core-flood data with the 30-wt% FM solution with the initial pH of 7.0 for investigating its performance under dynamic conditions.

Core floods

Flooding results. Figure 11 presents the cumulative oil recovery factors from the core floods with the brine, 20-wt% FM solution, and 30-wt% FM solution, all with the initial pH of 7.0. The water breakthrough occurred at 0.194, 0.221 and 0.229 PVI for the brine, 20-wt% FM, and 30-wt% FM cases, respectively. The oil recovery factor was 38.1% at the water breakthrough for the brine case, 42.2% for the 20-wt% FM case, and 44.0% for the 30-wt% FM case. The final oil recovery factors were nearly the same for the three cases as expected from the IFT data (Table 1). The two FM solution cases delayed the water breakthrough and improved the displacement efficiency at early times. As shown in the next subsection, these results were used to quantify the wettability alteration for the two FM solution cases.

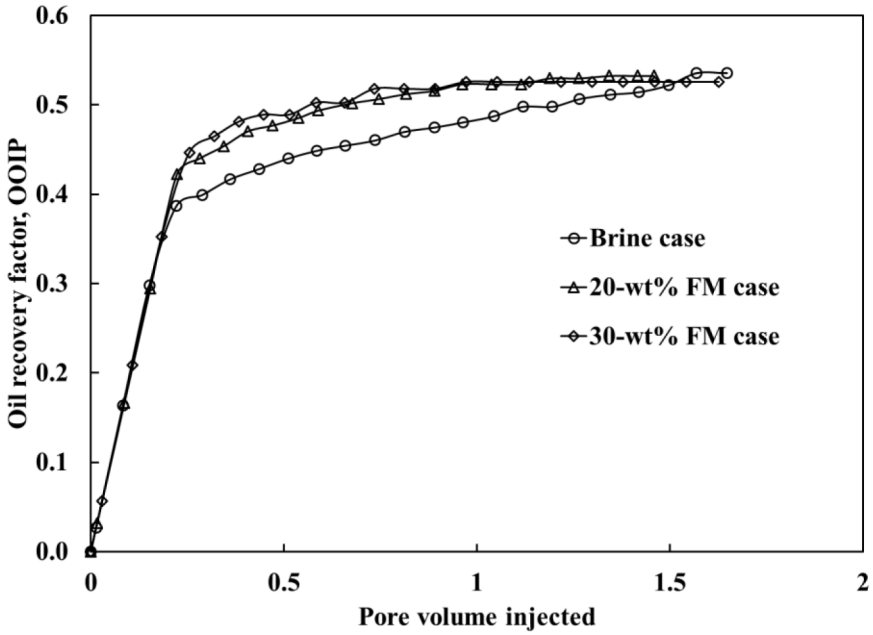

Figure 11—Cumulative oil recovery factors (PV) from core floods (Section 3.3.1).

History matching. Figures 12 **and** 13 show the matching results of oil recovery and water cut, respectively. Figure 14 shows the relative permeability curves for three cases after history matching. The relative permeability was calculated by dividing the effective permeability by oil permeability at initial water saturation in this figure. These relative permeability curves were then used to evaluate the core-scale wettability using the Lak and modified Lak wettability indices.

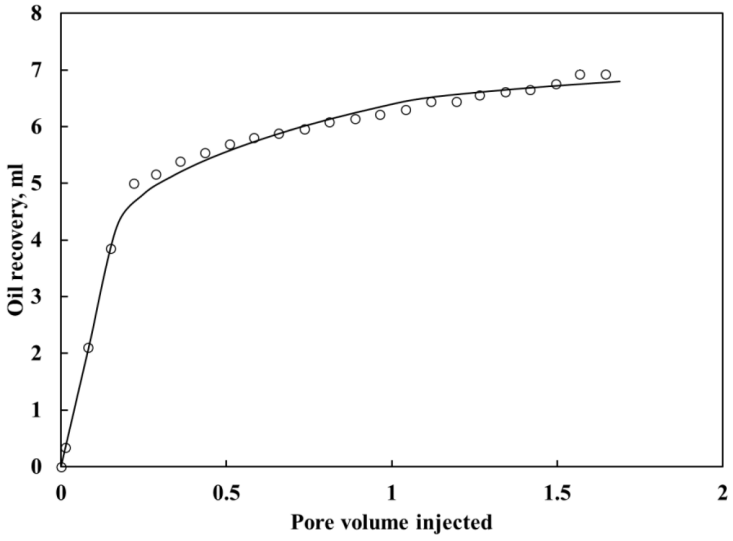

(A)

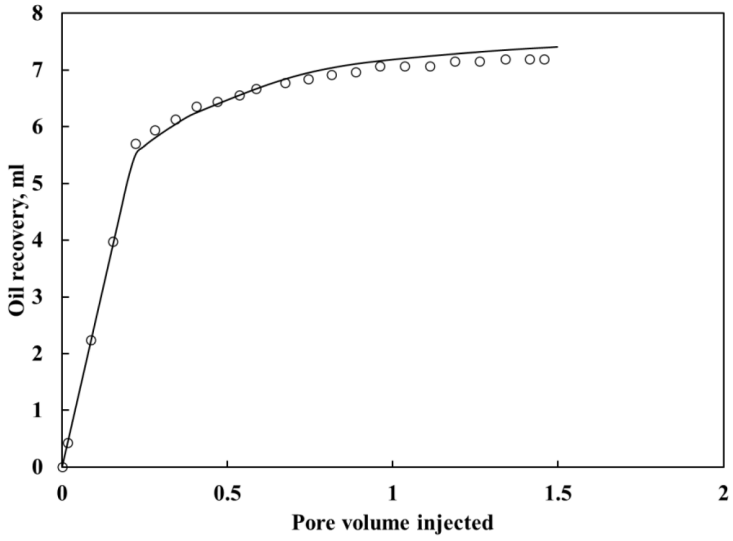

(B)

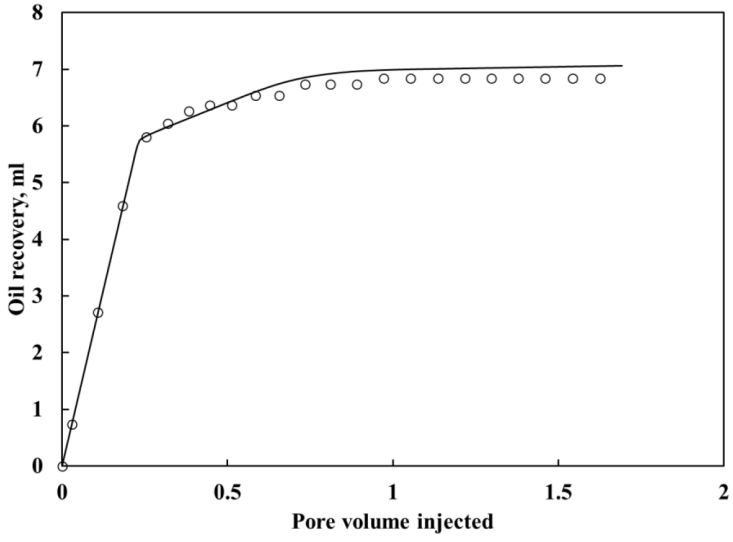

(C)

Figure 12—Matching results of oil recovery for (A) brine case, (B) 20-wt % FM case, and (C) 30-wt% FM case all with the initial pH of 7.0 (Section 3.3.2).

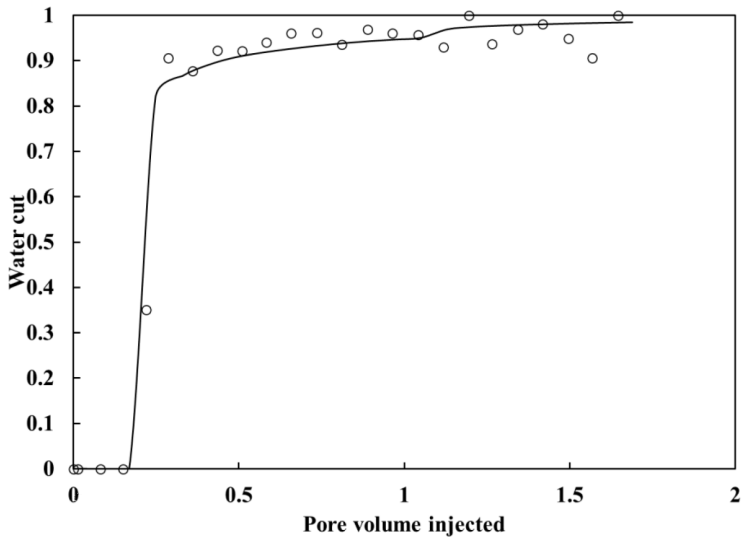

(A)

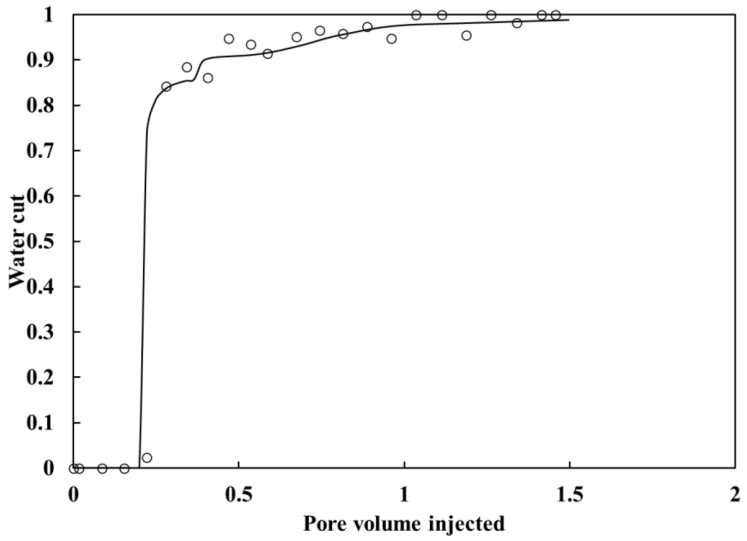

(B)

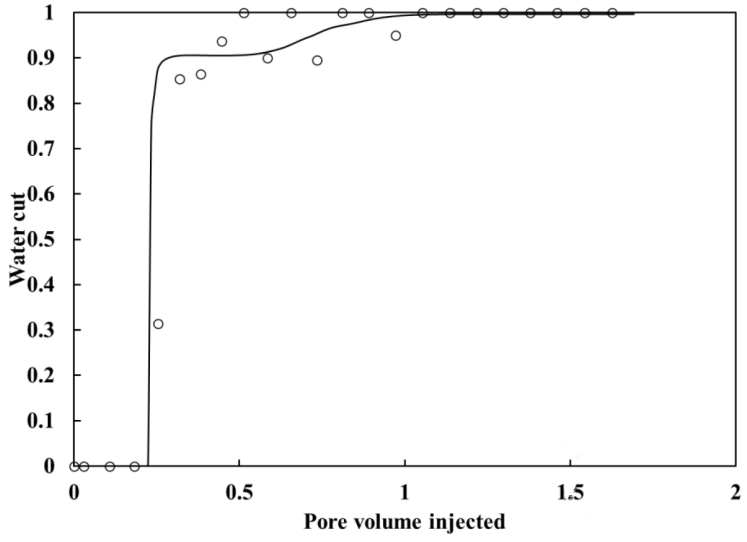

(C)

Figure 13—Matching results of water cut for (A) brine case, (B) 20-wt% FM case, and (C) 30-wt% FM case all with the initial pH of 7.0 (Section 3.3.2).

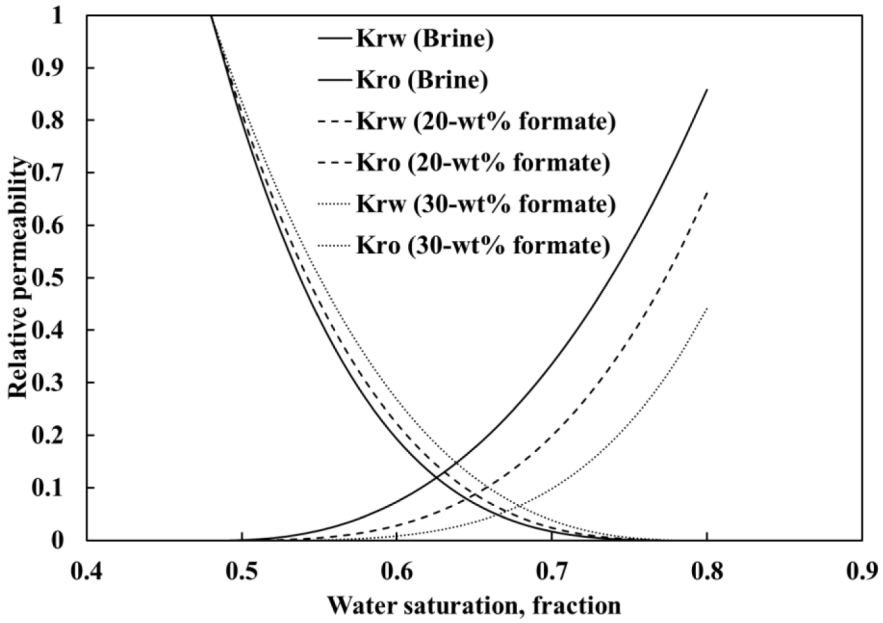

Figure 14—Relative permeability curves obtained from history matching of the core flooding data (Section 3.3.2). Table 7 shows the analysis of these relative permeability curves for the Lak wettability indices.

Table 7 shows these indices calculated based on the history-matched relative permeabilities. Two indices for the brine case had negative values (-0.43 and -0.19); that is, the rock was oil wet. For the 20-wt% FM case, the Lak wettability index was -0.17 and the modified Lak wettability index was 0.07. These values near zero indicate that the rock was intermediate wet. For the 30-wt% FM case, both wettability indices were positive (i.e., 0.08 and 0.40) and, therefore, the rock was water-wet. This quantitative analysis revealed the extent of the wettability changes after the injection of FM solution towards a more water-wet state. Figure 15 confirmed that the consistency between the two indices with a clear positive correlation. Note that the viscosities for the three injection solutions were different and properly modeled in the numerical simulations; therefore, the effect of the displacing fluid viscosity on the water breakthrough time was separated from that of wettability alteration in this analysis.

Table 7—Lak and modified Lak wettability indices calculated for the calibrated relative permeabilities using the core flooding data (Section 3.3.2). All solutions had the initial pH of 7.0.

	Lak wettability index	Modified Lak wettability index
Brine	−0.43	−0.19
20-wt% FM	−0.17	0.07
30-wt% FM	0.08	0.40

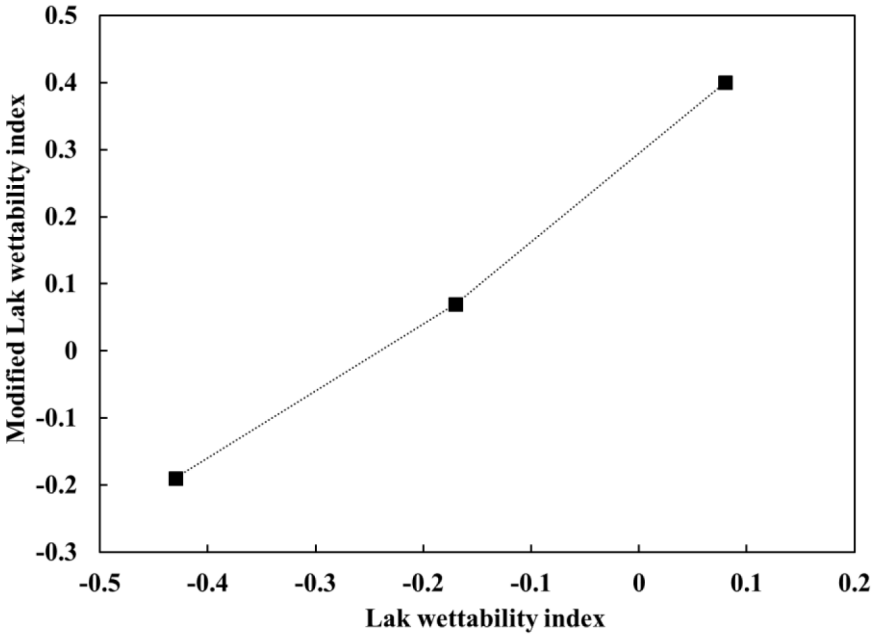

Figure 15—Lak wettability indices and modified Lak wettability indices in Table 7 show the consistency with a clear positive correlation (Section 3.3.2).

Carbon storage calculation. Lastly, the calibrated simulation model was used to indicate the amount of carbon storage for the core floods with the FM solutions (20-wt% and 30-wt%). The volume balance gives that the produced oil volume was equal to the volume of FM solution that retained in the core. Hence, the following equation gives the carbon amount that took the place of in-situ oil:

$$C_j = \frac{V_o \rho_{FM} c_{FM}}{MW} \tag{10}$$

where c_j is the amount of carbon stored by FM, V_o is the produced oil volume, ρ_{FM} is the density of FM solution, c_{FM} is the mass concentration of FM, and MW is the molecular weight of FM. Figure 16 shows that 20 and 30% FM solutions resulted in 9% and 15% carbon storage in place of in-situ oil, respectively. Note, however, that the reduction in carbon intensity of oil recovery by injection of FM solution would be different for different initial water saturations (e.g., secondary and tertiary oil recovery).

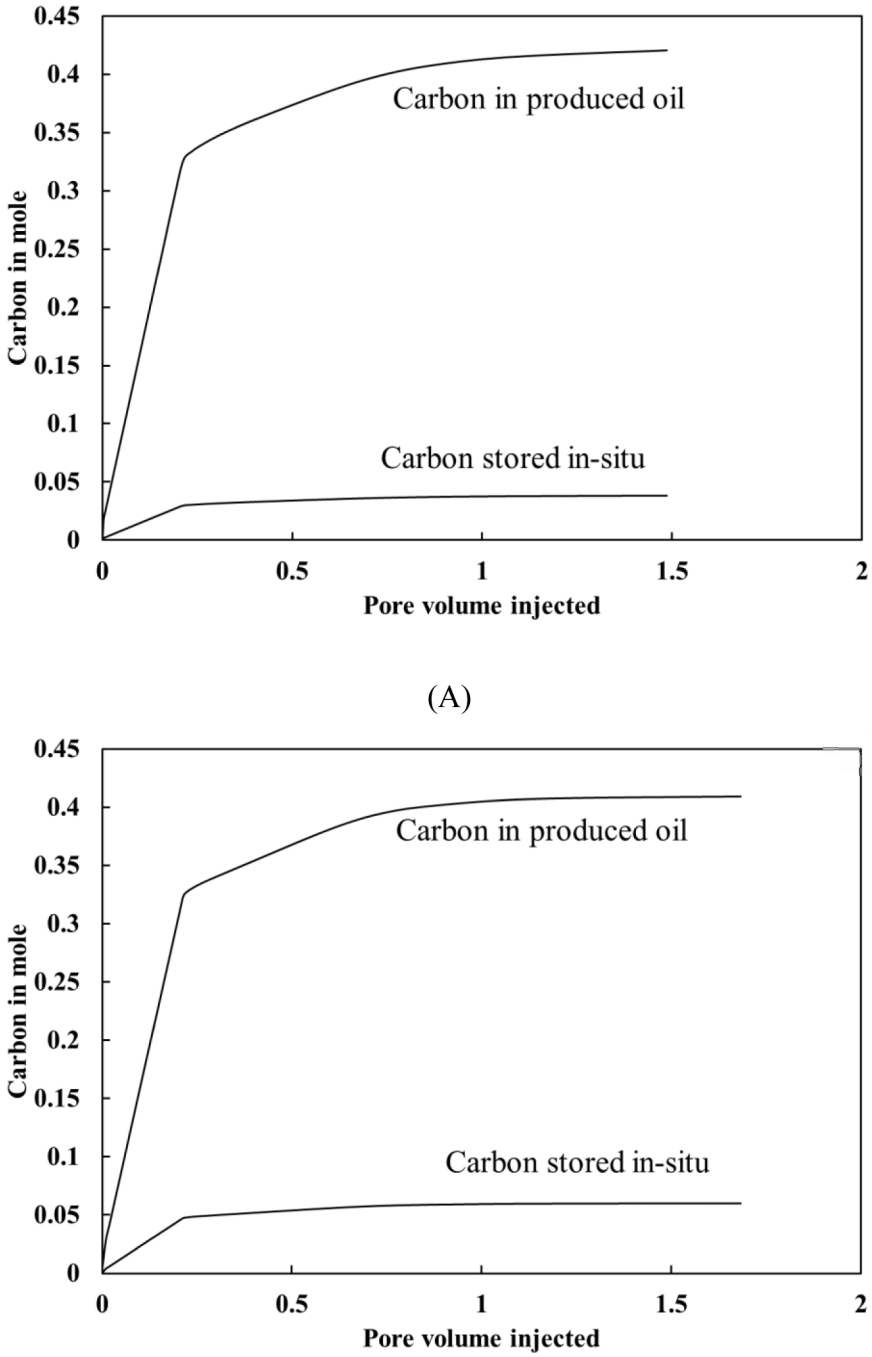

Figure 16—The amount of carbon produced by oil recovery and that of storage as FM based on the calibrated simulation models for 20-wt% formate (A) and 30-wt% formate (B) solution cases.

Discussion

The local measurements of contact angle on calcite chips were conducted as part of this research. However, the results were less conclusive than core-scale data, such as Amott wettability test and core flooding, mainly because the calcite dissolution by the formate solutions led to the effervescence of CO_2 gas bubbles. Various types of variability in surface properties, such as surface roughness and surface heterogeneity, often makes contact angle inconclusive as reported in the literature (Chau et al., 2009; Kung et al., 2019). The inherent difficulty of local contact angle measurements was coupled with CO_2 bubbles caused by the calcite

dissolution with high-concentration FM solutions in this research. In particular, the effervescence of CO_2 bubbles made it impossible for the oil droplets to adhere to the rock surface when placed in the 30-wt% FM solutions (the initial pH 6.1 and 7.0). The oil films on the oil-aged calcite chips placed in the two 30-wt% FM solutions were completely washed off the surface.

Baghishov et al. (2022) proposed that the wettability alteration by FM occurs because of the calcite dissolution caused by a slightly reduced pH and adsorption of FM ions on calcite-rich surfaces. In this research, a substantial level of calcite dissolution was confirmed even at a neutral pH because of the complexation of calcium and FM ions with the 30-wt% FM solution. Then, the reduction in the initial solution pH (from 7.0 to 6.1) substantially enhanced the wettability alteration of the core because the solution pH affected the charge of the calcite surface. The surface charge dictates the adsorption and desorption reactions that happen near the surface. Therefore, the wettability alteration observed in this research can be explained via charge interactions on the calcite surface. As schematically shown in Figure 17, one potential scenario is described below.

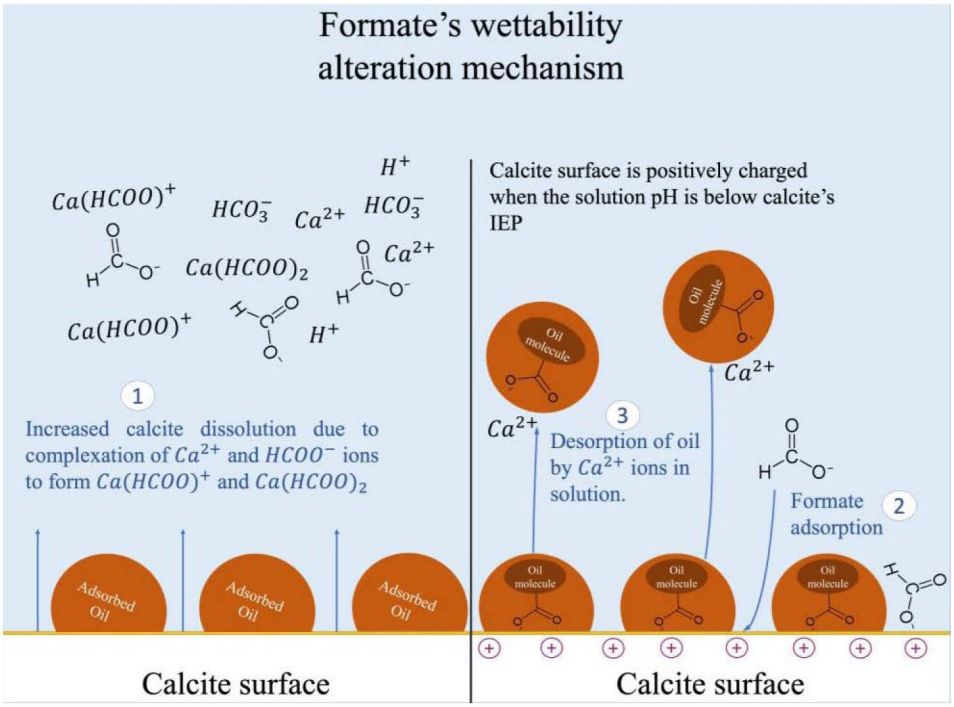

Figure 17—Suggested wettability alteration mechanism by formate in carbonates. The calcite surface is positively charged when the pH is sufficiently lower than the surface IEP. A positively charged calcite surface is likely the key to initiating formate adsorption and the oil desorption process by calcium ions (Bai et al. 2020; Zhang et al. 2007).

First, the FM imbibition increased calcite dissolution due to the formation of calcium-FM complexes. When the solution pH (e.g., 6.1) was sufficiently below the calcite isoelectric point, the FM ion in the solution adsorbed on the positively charged calcite surface. Then, the FM adsorption reduced the repulsion between the positively charged calcite surface and the calcium ions in solution, allowing for the calcium ions in solution got closer to the calcite surface. The calcium ions in solution were then able to desorb the adsorbed oil film from the surface of the rock (Bai et al. 2020; Zhang et al. 2007).

Conclusions

This paper presented a new set of experimental data regarding the core-scale wettability alteration of carbonate porous media with varying concentration (up to 30 wt%) of FM in NaCl brine. The experiments included Amott wettability tests (spontaneous and forced displacements) and core flooding experiments

along with static calcite dissolution tests. Experimental data were analyzed through geochemical modeling and numerical history-matching for mechanistic understanding of the wettability alteration observed in the experiments. The main conclusions are as follows:

- The static calcite dissolution tests showed that the degree of calcite dissolution increased with increasing FM concentration in the brine even with the initially neutral pH. For example, the calcium concentration in the 30-wt% FM case was 15.9 times greater than that in the brine case with the initial pH of 7.0. Furthermore, reducing the initial solution pH from 7.0 to 6.1 for the 30-wt% FM solution caused the calcium ion concentration to increase by a factor of 3.2. Geochemical modeling showed that the increased calcite dissolution could be caused by the formation of calcium FM complexes that reduced the activity coefficient of the calcium ion and therefore, drove the calcite dissolution.
- The 30-wt% FM solution with the initial pH of 6.1 yielded 4.7 times greater oil recovery than the brine case in the spontaneous imbibition, resulting in the Amott index of 0.39, which is approximately three times greater than that of the brine case. This clearly indicates the wettability alteration by the FM solution.
- The 30-wt% FM solution with the initial pH of 7.0 yielded only 30% greater oil recovery than the brine case in the spontaneous imbibition; however, it reached nearly the same amount of total oil recovery (spontaneous and forced) with the 30-wt% FM solution with the initial pH of 6.1. Therefore, the Amott index for this case, 0.12, may be misleading since the in-situ solution pH could be sufficiently lower than the calcite isoelectric point consistently in the forced-imbibition stage, unlike under the static conditions during the spontaneous-imbibition stage.
- Flooding experiments for Indiana limestone cores with FM solutions showed that increasing the FM concentration in the injected solution delayed the water breakthrough. Since FM did not substantially reduce the IFT of the solution with oil, the ultimate oil recovery did not change with the addition of FM into the injection brine. Numerical history matching of the core flooding data showed that increasing the FM concentration in the injected brine rendered the initially oil-wet core to a more water-wet state as quantified by Lak and modified Lak wettability indices.
- The wettability alteration by the 30-wt% FM solution with the initial pH of 7.0 was clear in core flooding experiments, including the forced-displacement part of the Amott wettability test, but unclear under static conditions in the spontaneous-imbibition stage of the Amott wettability test. This indicates the importance of in-situ solution pH in wettability alteration by aqueous FM solution in carbonate media, in order to cause the rock surface to be positively charged in the presence of FM and calcium ions.

Acknowledgement

We acknowledge the support of JX Nippon Oil & Gas Exploration for this research along with sponsors of the Energi Simulation Industrial Affiliate Program on Carbon Utilization and Storage (ES Carbon UT) at the Center for Subsurface Energy and the Environment at the University of Texas at Austin. Ryosuke Okuno holds the Pioneer Corporation Faculty Fellowship in the Hildebrand Department of Petroleum and Geosystems Engineering at The University of Texas at Austin.

References

Agarwal, A. S., Zhai, Y., Hill, D. et al. 2011. The Electrochemical Reduction of Carbon Dioxide to Formate/Formic Acid: Engineering and Economic Feasibility. *ChemSusChem*, **4**(9): 1301-1310. https://doi.org/10.1002/cssc.201100220

Akbar, M., Vissapragada, B., Alghamdi, A. H. et al. 2000. A Snapshot of Carbonate Reservoir Evaluation. *Oilfield Review* **12**(4), 20–21.

Al Mahrouqi, D., Vinogradov, J., and Jackson, M. D. 2017. Zeta Potential of Artificial and Natural Calcite in Aqueous Solution. *Advances in Colloid and Interface Science* **240**: 60-76. https://doi.org/10.1016/j.cis.2016.12.006

Alarji, H., Alazman, A., and Regenauer-Lieb, K. 2022. The Impact of Effective Tortuosity on Carbonate Acidizing and the Validation of Damköhler and Péclet Dimensionless Phase Space. *Journal of Petroleum Science and Engineering* **212**: 110313. https://doi.org/10.1016/j.petrol.2022.110313

Allison, J.D.; Brown, D.S.; Novo-Gradac, K.J. 1990. MINTEQA2/PRODEFA2—A Geochemical Assessment Model for Environmental Systems—Version 3.0 User's Manual; Environmental Research Laboratory, Office of Research and Development U.S. Environmental Protection Agency: Athens, GA, USA, 1990.

Anderson, W. G. 1986. Wettability Literature Survey-Part 1: Rock/Oil/Brine Interactions and the Effects of Core Handling on Wettability. *Journal of Petroleum Technology* **38**(10): 1125-1144. SPE-13932-PA. https://doi.org/10.2118/13932-PA

Argüelles-Vivas, F. J., Wang, M., Abeykoon, G. A. et al. 2020. Oil Recovery from Fractured Porous Media with/without Initial Water Saturation by Using 3-Pentanone and its Aqueous Solution. *Fuel* **276**: 118031. https://doi.org/10.1016/j.fuel.2020.118031

Baghishov, I., Abeykoon, G. A., Wang, M. et al. 2022. A Mechanistic Comparison of Formate, Acetate, and Glycine as Wettability Modifiers for Carbonate and Shale Formations. *Colloids and Surfaces A: Physicochemical and Engineering Aspects* **652**: 129849. https://doi.org/10.1016/j.colsurfa.2022.129849

Bai, S., Kubelka, J., and Piri, M. 2020. A Positively Charged Calcite Surface Model for Molecular Dynamics Studies of Wettability Alteration. *Journal of Colloid and Interface Science* **569**: 128-139. https://doi.org/10.1016/j.jcis.2020.02.037

Bai, S., Kubelka, J., and Piri, M. 2021. Wettability Alteration by Smart Water Multi-ion Exchange in Carbonates: A Molecular Dynamics Simulation Study. *Journal of Molecular Liquids* **332**: 115830. https://doi.org/10.1016/j.molliq.2021.115830

Busscher, H. J., Van Pelt, A. W. J., De Boer, P. et al. 1984. The Effect of Surface Roughening of Polymers on Measured Contact Angles of Liquids. *Colloids and Surfaces* **9**(4): 319-331. https://doi.org/10.1016/0166-6622(84)80175-4

Carrell, C. J., Carrell, H. L., Erlebacher, J. et al. 1988. Structural Aspects of Metal Ion Carboxylate Interactions. *Journal of the American Chemical Society* **110**(26): 8651-8656. https://doi.org/10.1021/ja00234a011

Chau, T. T., Bruckard, W. J., Koh, P. T. L. et al. 2009. A Review of Factors that Affect Contact Angle and Implications for Flotation Practice. *Advances in Colloid and Interface Science* **150**(2): 106-115. https://doi.org/10.1016/j.cis.2009.07.003

Clegg, S. L. 2018. Activity coefficients in natural waters. In *Activity Coefficients in Electrolyte Solutions* (pp. 279-434). CRC Press.

Computer Modelling Group, 2018. STARS Version 2018 User's Guide. Computer Modelling Group, Calgary, Alberta, Canada.

Deerfield, D. W., Lapadat, M. A., Spremulli, L. L. et al. 1989. The Role of Hydrated Divalent Metal Ions in the Bridging of Two Anionic Groups. An Ab Initio Quantum Chemical and Molecular Mechanics Study of Dimethyl Phosphate and Formate Bridged by Calcium and Magnesium Ions. *Journal of Biomolecular Structure and Dynamics* **6**(6): 1077-1091. https://doi.org/10.1080/07391102.1989.10506538

Deng, X., Kamal, M. S., Patil, S. et al. 2019. A Review on Wettability Alteration in Carbonate Rocks: Wettability modifiers. *Energy & Fuels* **34**(1): 31-54. https://doi.org/10.1021/acs.energyfuels.9b03409

Downs, J.D. 1993. Formate Brines: Novel Drilling and Completion Fluids for Demanding Environments. Paper presented at the SPE International Symposium on Oilfield Chemistry, New Orleans, Louisiana, March 1993. SPE-25177-MS. https://doi.org/10.2118/25177-MS

European Commission CORDIS. (2022, May 26). Oxalic Acid from CO2 Using Electrochemistry at Demonstration scale. https://doi.org/10.3030/767798

Giebson, C., Seyfarth, K., and Stark, J. 2010. Influence of Acetate and Formate-based Deicers on ASR in Airfield Concrete Pavements. *Cement and Concrete Research* **40**(4): 537-545. https://doi.org/10.1016/j.cemconres.2009.09.009

Gupta, R., and Mohanty, K. K. 2010. Temperature Effects on Surfactant-aided Imbibition into Fractured Carbonates. *SPE J.* **15**(03): 588-597. SPE-110204-PA. https://doi.org/10.2118/110204-PA

Harimi, B., Masihi, M., Mirzaei-Paiaman, A. et al. 2019. Experimental Study of Dynamic Imbibition during Water Flooding of Naturally Fractured Reservoirs. *Journal of Petroleum Science and Engineering* **174**: 1-13. https://doi.org/10.1016/j.petrol.2018.11.008

Hietala, J., Vuori, A., Johnsson, P. et al. 2016. Formic Acid. In *Ullmann's Encyclopedia of Industrial Chemistry*, (Ed.). https://doi.org/10.1002/14356007.a12_013.pub3

Hiorth, A., Cathles, L. M., and Madland, M. V. 2010. The Impact of Pore Water Chemistry on Carbonate Surface Charge and Oil Wettability. *Transport in porous media* **85**: 1-21. https://doi.org/10.1007/s11242-010-9543-6

Howard, S. K. 1995. Formate Brines for Drilling and Completion: State of the Art. SPE Annual Technical Conference and Exhibition, Dallas, Texas, October 1995. SPE-30498-MS. https://doi.org/10.2118/30498-MS

IEA (2021), Greenhouse Gas Emissions from Energy Data Explorer, IEA, Paris https://www.iea.org/data-and-statistics/data-tools/greenhouse-gas-emissions-from-energy-data-explorer

IEA (2022), World Energy Outlook 2022, IEA, Paris https://www.iea.org/reports/world-energy-outlook-2022, License: CC BY 4.0 (report); CC BY NC SA 4.0 (Annex A)

Kung, C. H., Sow, P. K., Zahiri, B. et al. 2019. Assessment and Interpretation of Surface Wettability Based on Sessile Droplet Contact Angle Measurement: Challenges and Opportunities. *Advanced Materials Interfaces* **6**(18): 1900839. https://doi.org/10.1002/admi.201900839

Lake, L., Johns, R. T., Rossen, W. R. et al. 2014. *Fundamentals of Enhanced Oil Recovery*. Richardson, Texas, USA: *Society of Petroleum Engineers*.

Lara Orozco, R.A., Abeykoon, G.A., Wang, M., et al. 2020. Amino Acid as a Novel Wettability Modifier for Enhanced Waterflooding in Carbonate Reservoirs. *SPE Reservoir Evaluation & Engineering*, **23**(02): 741 – 757. https://doi.org/10.2118/195907-PA

Mahani, H., Keya, A. L., Berg, S. et al. 2015. Insights into the Mechanism of Wettability Alteration by Low-Salinity Flooding (LSF) in Carbonates. *Energy & Fuels* **29**(3): 1352-1367. https://doi.org/10.1021/ef5023847

Mason, G., and Morrow, N. R. 2013. Developments in Spontaneous Imbibition and Possibilities for Future Work. *Journal of Petroleum Science and Engineering* **110**: 268-293. https://doi.org/10.1016/j.petrol.2013.08.018

Meng, Q., Liu, H., Wang, J. et al. 2016. Effect of Gravity on Spontaneous Imbibition from Cores with Two Ends Open in the Frontal Flow Period. *Journal of Petroleum Science and Engineering* **141**: 16-23. https://doi.org/10.1016/j.petrol.2016.01.024

Mirzaei-Paiaman, A. 2015. Analysis of Counter-current Spontaneous Imbibition in Presence of Resistive Gravity Forces: Displacement Characteristics and Scaling. *Journal of Unconventional Oil and Gas Resources* **12**: 68-86. https://doi.org/10.1016/j.juogr.2015.09.001

Mirzaei-Paiaman, A. 2021. New Methods for Qualitative and Quantitative Determination of Wettability from Relative Permeability Curves: Revisiting Craig's Rules of Thumb and Introducing Lak Wettability Index. *Fuel* **288**: 119623. https://doi.org/10.1016/j.fuel.2020.119623

Mirzaei-Paiaman, A., and Masihi, M. 2013. Scaling Equations for Oil/Gas Recovery from Fractured Porous Media by Counter-Current Spontaneous Imbibition: From Development to Application. *Energy & Fuels* **27**(8): 4662-4676. https://doi.org/10.1021/ef400990p

Mirzaei-Paiaman, A., Faramarzi-Palangar, M., Djezzar, S. et al. 2022. A New Approach to Measure Wettability by Relative Permeability Measurements. *Journal of Petroleum Science and Engineering* **208**: 109191. https://doi.org/10.1016/j.petrol.2021.109191

Mirzaei-Paiaman, A., Kord, S., Hamidpour, E. et al. 2017. Scaling One-and Multi-dimensional Co-Current Spontaneous Imbibition Processes in Fractured Reservoirs. *Fuel* **196**: 458-472. https://doi.org/10.1016/j.fuel.2017.01.120

Mirzaei-Paiaman, A., Masihi, M., and Standnes, D. C. 2013. Index for Characterizing Wettability of Reservoir Rocks based on Spontaneous Imbibition Recovery Data. *Energy & Fuels* **27**(12): 7360-7368. https://doi.org/10.1021/ef401953b

Morrow, N. R. 1975. The Effects of Surface Roughness on Contact Angle with Special Reference to Petroleum Recovery. *Journal of Canadian Petroleum Technology* **14**(04). PETSOC-75-04-04. https://doi.org/10.2118/75-04-04

Morrow, N. R. 1990. Wettability and its Effect on Oil Recovery. *Journal of Petroleum Technology* **42**(12): 1476-1484. SPE-21621-PA. https://doi.org/10.2118/21621-PA

Oyenowo, O. P., Sheng, K., and Okuno, R. 2023. Simulation Case Studies of Aqueous Formate Solution for Geological Carbon Storage. *Fuel* **334**: 126643. https://doi.org/10.1016/j.fuel.2022.126643

Parkhurst, D.L., and Appelo, C.A.J., 2013. Description of Input and Examples for PHREEQC version 3—A computer program for speciation, batch-reaction, one-dimensional transport, and inverse geochemical calculations: U.S. Geological Survey Techniques and Methods, book 6, chap. A43, 497 p., https://doi.org/10.3133/tm6A43

Philips, M. F., Gruter, G. J. M., Koper, M. T. et al. 2020. Optimizing the Electrochemical Reduction of CO2 to Formate: A State-of-the-Art Analysis. *ACS Sustainable Chemistry & Engineering* **8**(41): 15430-15444. https://doi.org/10.1021/acssuschemeng.0c05215

Pierre, A., Lamarche, J. M., Mercier, R. et al. 1990. Calcium as Potential Determining Ion in Aqueous Calcite Suspensions. *JOURNAL OF DISPERSION SCIENCE ANDTECHNOLOGY* **11**(6): 611-635. https://doi.org/10.1080/01932699008943286

Pitzer, K. S., & Press, C. R. C. (Eds.). 1991. Activity Coefficients in Electrolyte Solutions (Vol. **2**). Boca Raton, FL: CRC press.

Rapoport, L. A., and Leas, W. J. 1953. Properties of Linear Waterfloods. *Journal of Petroleum Technology* **5**(05): 139-148. SPE-213-G. https://doi.org/10.2118/213-G

Rostami Ravari, R., Strand, S., and Austad, T. 2011. Combined Surfactant-Enhanced Gravity Drainage (SEGD) of Oil and the Wettability Alteration in Carbonates: The Effect of Rock Permeability and Interfacial Tension (IFT). *Energy & Fuels* **25**(5): 2083-2088. https://doi.org/10.1021/ef200085t

Schechter, D. S., Zhou, D., and Orr Jr, F. M. 1994. Low IFT Drainage and Imbibition. *Journal of Petroleum Science and Engineering* **11**(4): 283-300. https://doi.org/10.1016/0920-4105(94)90047-7

Sohrabi, M., Riazi, M., Jamiolahmady, M. et al. 2011. Carbonated Water Injection (CWI)–A Productive Way of Using CO2 for Oil Recovery and CO2 storage. *Energy Procedia* **4**: 2192-2199. https://doi.org/10.1016/j.egypro.2011.02.106

Somasundaran, P., and Agar, G. E. 1967. The Zero Point of Charge of Calcite. *Journal of Colloid and Interface Science* **24**(4): 433-440. https://doi.org/10.1016/0021-9797(67)90241-X

Standnes, D. C., and Austad, T. 2003. Wettability Alteration in Carbonates: Interaction between Cationic Surfactant and Carboxylates as a Key Factor in Wettability Alteration from Oil-Wet to Water-Wet Conditions. *Colloids and Surfaces A: Physicochemical and Engineering Aspects* **216**(1-3): 243-259. https://doi.org/10.1016/S0927-7757(02)00580-0

Strand, S., Høgnesen, E. J., and Austad, T. 2006. Wettability Alteration of Carbonates—Effects of Potential Determining Ions (Ca2+ and SO42–) and Temperature. *Colloids and Surfaces A: Physicochemical and Engineering Aspects* **275**(1-3): 1-10. https://doi.org/10.1016/j.colsurfa.2005.10.061

U.S. Environmental Protection Agency. MINTEQA2/PRODEFA2, A Geochemical Assessment Model for Environmental Systems—User Manual Supplement for Version 4.0; National Exposure Research Laboratory, Ecosystems Research Division: Athens, GA, USA, 1998.

Wang, H., Oyenowo, O.P., and Okuno, R. 2023. Aqueous Formate Solution for Enhanced Water Imbibition in Oil Recovery and Carbon Storage in Carbonate Reservoirs [Under review]. *Fuel*

Wang, M., Abeykoon, G. A., Argüelles-Vivas, F. J. et al. 2022. Aqueous Solution of 3-Pentanone for Enhanced Oil Production from Tight Porous Media. *Journal of Petroleum Science and Engineering* **213**: 110376. https://doi.org/10.1016/j.petrol.2022.110376

Wang, M., Baek, K. H., Abeykoon, G. A. et al. 2019. Comparative Study of Ketone and Surfactant for Enhancement of Water Imbibition in Fractured Porous Media. *Energy & Fuels* **34**(5): 5159-5167. https://doi.org/10.1021/acs.energyfuels.9b03571

Wenzel, R. N. 1936. Resistance of Solid Surfaces to Wetting by Water. *Industrial & Engineering Chemistry* **28**(8): 988-994. https://doi.org/10.1021/ie50320a024

Xiang, H., Miller, H. A., Bellini, M. et al. 2020. Production of Formate by CO2 Electrochemical Reduction and its Application in Energy Storage. *Sustainable Energy & Fuels* **4**(1): 277-284. https://doi.org/10.1039/C9SE00625G

Zeng, L., Chen, Y., Lu, Y. et al. 2020. Role of Brine Composition on Rock Surface Energy and its Implications for Subcritical Crack Growth in Calcite. *Journal of Molecular Liquids* **303**: 112638. https://doi.org/10.1016/j.molliq.2020.112638

Zhang, P., and Austad, T. 2006. Wettability and Oil Recovery from Carbonates: Effects of Temperature and Potential Determining Ions. *Colloids and Surfaces A: Physicochemical and Engineering Aspects* **279**(1-3): 179-187. https://doi.org/10.1016/j.colsurfa.2006.01.009

Zhang, P., Tweheyo, M. T., and Austad, T. 2007. Wettability Alteration and Improved Oil Recovery by Spontaneous Imbibition of Seawater into Chalk: Impact of the Potential Determining Ions Ca2+, Mg2+, and SO42–. *Colloids and Surfaces A: Physicochemical and Engineering Aspects* **301**(1-3): 199-208. https://doi.org/10.1016/j.colsurfa.2006.12.058

Zhang, S., Kang, P., and Meyer, T. J. 2014. Nanostructured Tin Catalysts for Selective Electrochemical Reduction of Carbon Dioxide to Formate. *Journal of the American Chemical Society* **136**(5): 1734-1737. https://doi.org/10.1021/ja4113885

Zheng, X., De Luna, P., de Arquer, F. P. G. et al. 2017. Sulfur-Modulated Tin Sites enable Highly Selective Electrochemical Reduction of CO2 to Formate. *Joule* **1**(4): 794-805. https://doi.org/10.1016/j.joule.2017.09.014

Appendix A.

Geochemistry model

This appendix contains the PHREEQC input file used in this research. The database sit.dat was used for all cases.

Figure A-1 shows an input script with the aqueous and ion-complexation equations defined in equations 4 and 5. The script is divided into keyword blocks with each having a separate function. The SOLUTION_SPREAD block was used to input the solution compositions. The SOLUTION_MASTER_SPECIES was used to define the FM ion molecular weight and valence state. The SOLUTION_SPECIES block was used to define FM complexation reactions and their thermodynamic constants. The PHASES block was used to define the solubility of calcium formate solid. The EQUILIBRIUM_PHASES block was used to specify the minerals or gases in equilibrium with the solution and their respective saturation index. The SOLUTION_MASTER_SPECIES, SOLUTION_SPECIES, and PHASES block were used in adding FM data to the model, all other reactions were already defined within the database.

```
SOLUTION_SPREAD
UNITS ppm
temp 70
Number  pH  Na  Cl  Formate
1   7   5902.5  9097.5  0
2   7   31447.83742 9097.5  50000
3   7   56993.17484 9097.5  100000
4   7   108083.8497 9097.5  200000
5   7   159174.5245 9097.5  300000
6   6.1 159174.5245 9097.5  300000


SOLUTION_MASTER_SPECIES
Formate     Formate-    0.0 45.018  45.018


SOLUTION_SPECIES
Formate- = Formate-
    log_k 0

H+ + Formate- = H(Formate)
    log_k   3.745
    delta_h 0.1674  kJ
    -gamma  0   0
        #                   Id:  3309831
        #        log K source:  NIST46.2
        #      Delta H source:  NIST46.2
        #T and ionic strength:
        #                   Id:  2109831
        #        log K source:  NIST46.2
        #      Delta H source:  NIST46.2
        #T and ionic strength:
Ca+2 + Formate- = Ca(Formate)+
    log_k   1.43
    delta_h 4.184   kJ
    -gamma  0   0
        #                   Id:  1509831
        #        log K source:  NIST46.2
        #      Delta H source:  NIST46.2
        #T and ionic strength:
Ca+2 + 2Formate- = Ca(Formate)2
    log_k   2.24
    delta_h -300.6  kJ
    -gamma  0   0
        #   log K source: Giebson et al. (2010)

PHASES
Ca(Formate)
    Ca(Formate)2    =   Ca+2 + 2Formate-
    log_k   -2.40
    delta_h 0   kJ



USE SOLUTION 6

EQUILIBRIUM_PHASES
Calcite 0.0  # saturation index , moles (default = 10 mol)
CO2(g)  -2.04

END
```

Figure A-1—PHREEQC input file